Preprint of the paper

"Application of Meshless Methods to the Analysis and Design of Grounding Systems"

I. Colominas, M. Chao, F. Navarrina, M. Casteleiro (1998)
En "Computational Mechanics: New Trends and Applications" (CD-ROM), Parte I: "Mathematical Modelling and Numerical Methods", Sección 6: "Meshless Methods". S.R. Idelsohn, E. Oñate, E. Dvorkin (Editors); CIMNE, Barcelona. (ISBN: 84-89925-15-1)

http://caminos.udc.es/gmni

COMPUTATIONAL MECHANICS
New Trends and Applications
S. Idelsohn, E. Oñate and E. Dvorkin (Eds.)

APPLICATION OF MESHLESS METHODS TO THE ANALYSIS AND DESIGN OF GROUNDING SYSTEMS

Ignasi Colominas, Mar Chao, Fermín Navarrina, and Manuel Casteleiro

E.T.S. de Ingenieros de Caminos, Canales y Puertos de La Coruña
Depto. de Métodos Matemáticos y de Representación
Universidad de La Coruña
Campus de Elviña, 15192 La Coruña, SPAIN
E-mail: colominas@iccp.udc.es, t_chao@iccp.udc.es, navarrina@iccp.udc.es, casteleiro@udc.es
Web page: http://www.udc.es/caminos/

Key words: Meshless Methods, MLS Interpolants, Electromagnetics, Grounding

Abstract.
Analysis and design of grounding systems of electrical installations involves computing the potential distribution in the earth and the equivalent resistance of the system[1,2]*. Several numerical formulations based on the Boundary Element Method have recently been derived for grounding grids embedded in uniform soils*[2,3,4] *and in stratified soils*[5]*, which feasibility has been demonstrated with its application to large earthing systems in a two-layer soil*[4]*.*
In cases of the analysis of grounding systems buried in more stratified soils or heterogeneous, the application of Boundary Element approaches can require a considerable computational effort. On the other hand, the specific geometry of earthing systems in practice (a grid of interconnected buried conductors) precludes the use of standard numerical techniques (such as finite elements or finite differences)[2,3]*, since discretization of the domain (the earth) is required and the obtention of sufficiently accurate results should imply unacceptable computing efforts.*
For these reasons, we have turned our attention to investigate the applicability of numerical formulations based on meshless methods[6,7] *for the grounding analysis. In this paper, a meshless technique based on the Moving Least Square method with a point collocation approach is proposed.*

1. INTRODUCTION

The application of numerical simulation in engineering problems has considerably increased in last decades with the advance in the numerical methods and the development of computer sciences. As new problems are proposed, more challenges appear in the computational mechanics field.

The huge development of numerical methods such as Finite Differences or Finite Elements has represented a significant improvement in this area. However, some difficulties have been reported when these standard numerical techniques are applied to some engineering applications, as for example the treatment of moving discontinuities (cracks, shock waves, etc.) and the high-speed impact problems, or the numerical simulation in material science (fracture treatment, erosion problems, etc.), in fluid mechanics or electromagnetics[6,8]. In most of these problems, since an efficient mesh is required in their discretization, the mesh generation process can imply a lot of difficulties and it frequently become the bottle neck of the problem (sometimes requiring more computational effort than the resolution itself).

For this reason, a family of numerical methods where meshes are unnecessary, "the meshless methods", has been proposed[6,9]. In general, the main objective of these methods is to obtain the approximated solution to a given problem only in terms of the information in some points of the domain without requiring an explicit element mesh nor, consequently, a connectivity matrix to perform the assembly of the coefficient matrix. The solution domain is formed by a set of nodal points with an associated subdomain integrated by the closest points. Thus, the approximation for each central node or "star node" is obtained with the information provided by its subdomain points, what means that a local approximation in each node is achieved[10].

Although the first meshless methods (such as the Smooth Particle Hydrodynamics, SPH) were developed twenty years ago in the computational physics field[11,12], the more important theoretical research works about them (such as convergence or stability of the methods) and their application in computational mechanics have been recently performed[13].

Nayroles[14] proposed in 1992 the Diffuse Element Method (DEM), in which only a mesh of nodes and a boundary description is needed to formulate the Galerkin equations, the interpolants are polynomials fitted to the nodal values by a weighted least square approximation, and an auxiliar grid is used to compute the integral expressions derived from the Galerkin formulation. In 1994, Belystchko *et al.* modify and refine this technique, proposing the Element Free Galerkin Method (EFGM)[6,9,15].

Liu *et al.*[16,17] have recently proposed a different kind of meshless multiple scale methods (called Reproducing Kernel Particle methods, RKPM) based on reproducing kernels and wavelets techniques. The starting point of these methods is the SPH method, where several corrections and refinements have been introduced[13].

Other interesting and promising methods proposed in last years are the family of meshless techniques for the solution of boundary value problems, called *H-p* Cloud

Method[18,19]. It is based on the idea of constructing functions (h-p clouds) which allow the implementation of p and h-p adaptivity and can represent polynomials of any degree.

Oñate and other authors[7,8,20] have recently proposed a method which combines the moving least square approximation with a Point Collocation approach to compute the integral terms. This method completely avoids the necessity of mesh generation, because no auxiliary grid is required. Furthermore, different techniques can be derived if the weighting function is fixed (Diffuse Least Square Method, DLS) or it depends on the point where the approximated value is computed (Moving Least Square Method, MLS).

In this paper, a modified MLS method is proposed for the numerical solution of problems in computational mechanics. This method combines a moving least square approach using base interpolating functions normalized within each subdomain, with a Point Collocation scheme, and it is used for solving potential problems in electrical engineering applications.

2. MESHLESS METHODS BASED ON LEAST SQUARE APPROXIMATIONS

2.1 Overview of basic concepts

Let A and B be two differential operators, Ω the domain of our problem and Γ its boundary ($\Gamma = \Gamma_t \cup \Gamma_u$). In these terms, a scalar boundary value problem can be written as,

$$A(u) = b \qquad \text{in} \quad \Omega \tag{1}$$

with boundary conditions,

$$\begin{aligned} B(u) &= t \qquad \text{in} \quad \Gamma_{\mathrm{t}} \\ u - u_p &= 0 \qquad \text{in} \quad \Gamma_{\mathrm{u}} \end{aligned} \tag{2}$$

where u is the solution, b and t represent the actions over Ω and along the boundary Γ_t, and u_p is the prescribed value of u along Γ_u.

Application of weighted residual method allows to obtain a variational form of the above problem, in terms of the trial approximation function $\hat{u}$ of the unknown u, as

$$\int_\Omega \Psi_i \; [A(\hat{u}) - b] d\Omega + \int_{\Gamma_t} \widehat{\Psi}_i \; [B(\hat{u}) - t] d\Gamma + \int_{\Gamma_u} \widehat{\widehat{\Psi}}_i \; [\hat{u} - u_p] d\Gamma \; = \; 0 \tag{3}$$

which must hold for all members Ψ_i, $\widehat{\Psi}_i$ and $\widehat{\widehat{\Psi}}_i$ of suitable classes of test functions defined on Ω, Γ_t and Γ_u[21].

Now, for a given set of n_p trial functions $\{N_i\}$ defined on Ω, unknown $\hat{u}$ can be discretized in the form

$$u \cong \hat{u} = \sum_{i=1}^{n_p} N_i u_i^h = \boldsymbol{N}^t \boldsymbol{u}^h \tag{4}$$

being n_p the total number of nodal points of the solution domain, where the approximation is evaluated.

On the other hand, in order to preserve the local character of the approximation, functions $\{N_i\}$ must satisfy

$$\begin{array}{lll} N_i(\boldsymbol{x}) \neq 0 & \text{if} \ \boldsymbol{x} \in \Omega_{\mathrm{i}} \\ N_i(\boldsymbol{x}) = 0 & \text{if} \ \boldsymbol{x} \notin \Omega_{\mathrm{i}} \end{array} \tag{5}$$

where Ω_i is a subdomain of Ω containing n points ($n \ll n_p$).

Starting from this general statement, it is possible to derive specific formulations. Thus, different definitions of test functions allow to obtain for example the finite element, the finite difference and the finite volume methods[7].

2.2 Modified Moving Least Square Approximations

The basic idea of the Moving Least Square approximation is to replace the FEM interpolation, valid on an element, by a local weighted least square fitting, valid on a small neighbourhood of a point and based on its n closest points (domain Ω_k). The local character of the approximation comes from a moving weighting function which takes its maximum value at this point and vanishes outside a surrounding region.

In order to define properly the approximation at every point, it is necessary that all subdomains Ω_k cover all the interpolation domain. Hereby, these subdomains must overlap, and the common areas have to include enough nodal points in order to ensure the convergence of the method[22]. In the present paper, for a given nodal point (the "star" node) the selection of the nodal points included in its subdomain has been performed by using a simple an effective process based on the "four quadrants" technique[7].

If Ω_k is the interpolation domain of a function $u(\boldsymbol{x})$, it can be approximated by

$$u(\boldsymbol{x}) \cong \hat{u}(\boldsymbol{x}) = \sum_{i=1}^{m} p_i(\boldsymbol{x}) \alpha_i = \boldsymbol{p}^t(\boldsymbol{x}) \boldsymbol{\alpha} \tag{6}$$

where $\boldsymbol{\alpha} = [\alpha_1, \alpha_2, \ldots, \alpha_m]^t$ is a set of unknown coefficients, $\boldsymbol{p}(\boldsymbol{x})$ contains a base of interpolating functions (monomial terms, generally) which order is m.

In the approach presented in this paper, the base interpolating functions are normalized within each subdomain Ω_k by dividing for the maximum distance between the star point i of the domain and the surrounding points. Thus, we can define normalized coordinates ($\boldsymbol{\xi} \equiv [\xi, \eta, \zeta]$) within a subdomain Ω_k as,

$$\boldsymbol{\xi}(\boldsymbol{x}) = \left[\frac{x - x_i}{d}, \frac{y - y_i}{d}, \frac{z - z_i}{d} \right] \tag{7}$$

where d is the maximum distance between star node i and the points of its subdomain.

m	$1D$	$2D$	$3D$
1	$\boldsymbol{p}^t = [1]$	$\boldsymbol{p}^t = [1]$	$\boldsymbol{p}^t = [1]$
2	$\boldsymbol{p}^t = [1, \xi]$	–	–
3	$\boldsymbol{p}^t = [1, \xi, \xi^2]$	$\boldsymbol{p}^t = [1, \xi, \eta]$	–
4	–	–	$\boldsymbol{p}^t = [1, \xi, \eta, \zeta]$
6	–	$\boldsymbol{p}^t = [1, \xi, \eta, \xi^2, \xi\eta, \eta^2]$	–
10	–	–	$\boldsymbol{p}^t = [1, \xi, \eta, \zeta, \xi^2, \xi\eta, \eta^2, \eta\zeta, \zeta^2, \zeta\xi]$

Table 1— Normalized base interpolating functions (constant, lineal and quadratic).

On the other hand, function $u(\boldsymbol{x})$ can be sampled in the n points belonging to Ω_k as,

$$\boldsymbol{u}^h = \begin{pmatrix} u_1^h \\ u_2^h \\ \vdots \\ u_n^h \end{pmatrix} \cong \begin{pmatrix} \hat{u}_1 \\ \hat{u}_2 \\ \vdots \\ \hat{u}_n \end{pmatrix} = \begin{pmatrix} \boldsymbol{p}_1^t \\ \boldsymbol{p}_2^t \\ \vdots \\ \boldsymbol{p}_n^t \end{pmatrix} \boldsymbol{\alpha} = \boldsymbol{S}\boldsymbol{\alpha} \tag{8}$$

where u_j^h are the values of unknown function evaluated in nodal points of Ω_k ($u_j^h = u(\boldsymbol{x}_j)$, $j = 1, \ldots, n$), $\hat{u}_j = \hat{u}(\boldsymbol{x}_j)$ are their approximated values, and $\boldsymbol{p}_j$ contains the normalized base interpolating functions evaluated in $\boldsymbol{\xi}_j$ (where $\boldsymbol{\xi}_j = \boldsymbol{\xi}(\boldsymbol{x}_j)$). In table 1 we summarize base interpolating functions in 1D, 2D and 3D for constant, linear and quadratic order.

This result can be understood as a generalization of the finite element interpolation, since one obtains this approximation if the number of subdomain points n is chosen equal to order m of the polinomials base[23]. In this case, $\boldsymbol{S}$ in (8) is a square matrix, and shape functions $\boldsymbol{N}$ in (4) can be directly obtain combining (6) and (8).

In general, if $n > m$, $\boldsymbol{S}$ is a rectangular matrix and the approximation cannot fit all the u_j^h values. However, approximated values $\hat{u}(\boldsymbol{x})$ can be determined by minimizing the weighted sum of the square differences between the exact value u_j^h and the approximation $\hat{u}(\boldsymbol{x}_j)$ at each nodal point $\boldsymbol{x}_j$ belonging to the domain of node $\boldsymbol{x}_k$. The weighting

function is usually built in such a way that it equals unity in point $\boldsymbol{x}_k$ and vanishes outside domain Ω_k.

In the Moving Least Square approach, this functional can be written as

$$J(\boldsymbol{x}_k) = \sum_{j=1}^{n} \omega_k(\boldsymbol{x}_j, \boldsymbol{x}_k)(u_j^h - \hat{u}(\boldsymbol{x}_j))^2 = \sum_{j=1}^{n} \omega_k(\boldsymbol{x}_j, \boldsymbol{x}_k)(u_j^h - \boldsymbol{p}_j^t \boldsymbol{\alpha})^2 \tag{9}$$

where $\omega_k(\boldsymbol{x}_j, \boldsymbol{x}_k)$ is the weighting function computed in $\boldsymbol{x}_j$, which shape and span depend on $\boldsymbol{x}_k$. It must be pointed out that $\boldsymbol{x}_k$ represents an arbitrary position and can be replaced for the generic coordinate $\boldsymbol{x}$.

Now a standard minimization of (9) with respect to $\boldsymbol{\alpha}$

$$\frac{\partial J(\boldsymbol{x})}{\partial \alpha_i} = 0; \quad i = 1, m \tag{10}$$

results in

$$\boldsymbol{A}(\boldsymbol{x})\boldsymbol{\alpha} = \boldsymbol{B}(\boldsymbol{x})\boldsymbol{u}^h \tag{11}$$

being

$$\boldsymbol{A}(\boldsymbol{x}) = \sum_{j=1}^{n} \omega_k(\boldsymbol{x}_j, \boldsymbol{x})\boldsymbol{p}(\boldsymbol{\xi}_j)\boldsymbol{p}^t(\boldsymbol{\xi}_j) \tag{12}$$

$$\boldsymbol{B}(\boldsymbol{x}) = [\omega_k(\boldsymbol{x}_1, \boldsymbol{x})\boldsymbol{p}(\boldsymbol{\xi}_1)\,,\, \omega_k(\boldsymbol{x}_2, \boldsymbol{x})\boldsymbol{p}(\boldsymbol{\xi}_2)\,,\, \ldots\,,\, \omega_k(\boldsymbol{x}_n, \boldsymbol{x})\boldsymbol{p}(\boldsymbol{\xi}_n)] \tag{13}$$

where $\boldsymbol{\xi}_j = \boldsymbol{\xi}(\boldsymbol{x}_j)$, $j = 1, ..., n$.

These matrices may also be rewritten as,

$$\boldsymbol{A}(\boldsymbol{x}) = \boldsymbol{P}\boldsymbol{W}(\boldsymbol{x})\boldsymbol{P}^t \tag{14}$$

$$\boldsymbol{B}(\boldsymbol{x}) = \boldsymbol{P}\boldsymbol{W}(\boldsymbol{x}) \tag{15}$$

being auxiliary matrices $\boldsymbol{P}$ and $\boldsymbol{W}(\boldsymbol{x})$:

$$\boldsymbol{P} = [\boldsymbol{p}(\boldsymbol{\xi}_1) \quad \ldots \quad \boldsymbol{p}(\boldsymbol{\xi}_n)] \tag{16}$$

$$\boldsymbol{W}(\boldsymbol{x}) = diag\left[\omega_k(\boldsymbol{x}_j, \boldsymbol{x})\right], \quad j = 1, ..., n. \tag{17}$$

On the other hand, since $\boldsymbol{A}(\boldsymbol{x})$ is a square matrix, unknown coefficients $\boldsymbol{\alpha}$ yield from equation (11) as,

$$\boldsymbol{\alpha} = \boldsymbol{C}(\boldsymbol{x})\boldsymbol{u}^h \tag{18}$$

being $\boldsymbol{C}(\boldsymbol{x})$

$$\boldsymbol{C}(\boldsymbol{x}) = \boldsymbol{A}^{-1}(\boldsymbol{x})\boldsymbol{B}(\boldsymbol{x}) \tag{19}$$

Matrix $\boldsymbol{C}$ can be considered as the inverse of $\boldsymbol{S}$ in equation (8).

Now, the substitution of (18) in (6) allows to obtain an approximation to function $u(\boldsymbol{x})$ in Ω_k in the form,

$$u(\boldsymbol{x}) \cong \hat{u}(\boldsymbol{x}) = \boldsymbol{p}^t(\boldsymbol{\xi})\boldsymbol{C}(\boldsymbol{x})\boldsymbol{u}^h. \tag{20}$$

Therefore, shape functions are given by,

$$\boldsymbol{N}^t(\boldsymbol{x}) = \boldsymbol{p}^t(\boldsymbol{\xi})\boldsymbol{C}(\boldsymbol{x}). \tag{21}$$

It is important to remark that the local values of the approximating function do not fit the nodal unknown values,

$$\hat{u}(\boldsymbol{x}_j) \neq u_j^h \tag{22}$$

due to the least square character of the approximation. It must be pointed out that if $n = m$, the FEM type approximation is recovered and no effect of weighting is presented[7]. Besides, if the weighting function is constant and equals the unity, the standard least square method is reproduced.

2.3 Weighting Functions in MLS Approximation

Weighting functions play an important role in the performance of this kind of meshless methods. Depending on the definition of weighting functions one can obtain different least square methods. Thus, if a fixed function within every interpolation domain Ω_i is defined

$$\begin{aligned} &\omega_i(\boldsymbol{x}_i, \boldsymbol{x}_i) = 1, \quad i = 1, ..., n_p \\ &\omega_i(\boldsymbol{x}_i, \boldsymbol{x}) \neq 0, \quad \boldsymbol{x} \in \Omega_i \\ &\omega_i(\boldsymbol{x}_i, \boldsymbol{x}) = 0, \quad \boldsymbol{x} \notin \Omega_i, \end{aligned} \tag{23}$$

we obtain the Diffuse Least Square methods (DLS)[8].

In the Moving Least Square methods the weighting function is defined so that it is translated over the domain, and it is maximum over the position of interpolation point $\boldsymbol{x}_k$ (which subdomain is Ω_k) where function $\hat{u}$ is evaluated. In this case, the weighting function can be defined as

$$\begin{aligned} &\omega_k(\boldsymbol{x}_i, \boldsymbol{x}_k) = 1 \\ &\omega_k(\boldsymbol{x}_i, \boldsymbol{x}) \neq 0, \quad \boldsymbol{x} \in \Omega_k \\ &\omega_k(\boldsymbol{x}_i, \boldsymbol{x}) = 0, \quad \boldsymbol{x} \notin \Omega_k, \end{aligned} \tag{24}$$

In order to preserve its unique definition, the weighting function must be continuous and differentiable in Ω_k and vanish on its boundary and outside, ensuring that the number of n points within Ω_k is equal or greater than order m[7].

In general, the definition of a different weighting function for every interpolating point $\boldsymbol{x}_k$ is very difficult, presenting an infinite number of posibilities. To overcome this problem, we can define the weighting functions at nodal points $\boldsymbol{x}_i$, and use them evaluated in the arbitrary point $\boldsymbol{x}_k$. Therefore, $\omega_k(\boldsymbol{x}_i, \boldsymbol{x}_k)$ may be substituted by $\omega_i(\boldsymbol{x}_i, \boldsymbol{x}_k)$.

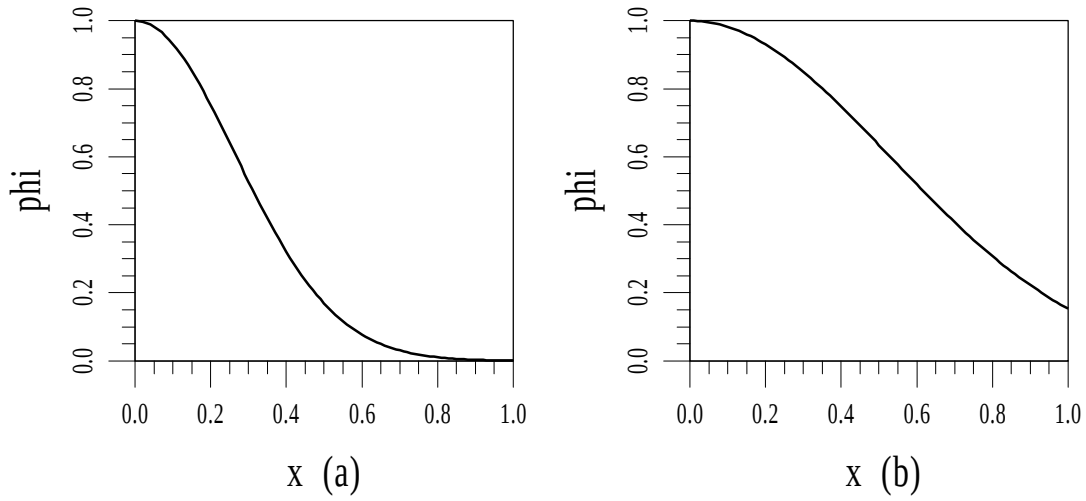

Figure 1.- Gaussian Weighting function for $d_{max} = 1.5\, max\|x - x_i\|$ and several values of α: a) $\alpha = 0.25$, b) $\alpha = 0.5$.

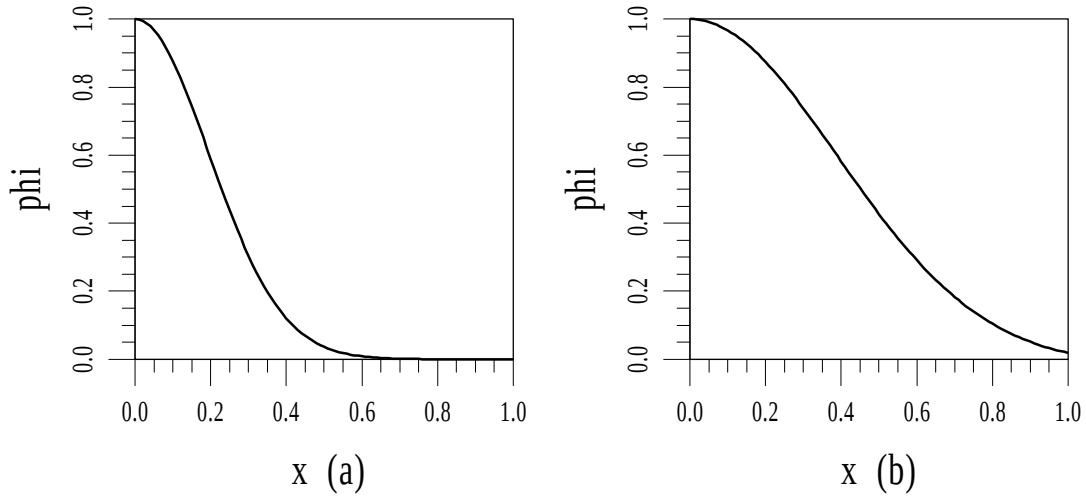

Figure 2.- Gaussian Weighting function for $d_{max} = 1.1 max\|x - x_i\|$ and several values of α: a) $\alpha = 0.25$, b) $\alpha = 0.5$.

Different kinds of weight functions have been proposed. In this paper we have considered two of the most common: the modified conoidal function and the truncated gaussian distribution. Thus, if we denote $\omega_i(\boldsymbol{x}_i, \boldsymbol{x}_k) = \phi_i(d)$ where d is the distance between nodal point $\boldsymbol{x}_i$ and arbitrary point $\boldsymbol{x}_k$ ($d = \|\boldsymbol{x}_i - \boldsymbol{x}_k\|$), the modified conoidal

weighting is

$$\phi_i(d) = \left[1 - \left(\frac{d}{d_{max}}\right)^2\right]^m \tag{25}$$

where the parameter m is usually chosen[23] as 4, and the truncated gaussian distribution is

$$\phi_i(d) = \frac{e^{-(\frac{d}{c})^2} - e^{-(\frac{d_{max}}{c})^2}}{1 - e^{-(\frac{d_{max}}{c})^2}} \tag{26}$$

where d_{max} is the domain of influence of the weight function in Ω_k and c is a constant value, which determines the shape of the weight function. The domain of influence is obtained by multiplying the maximum distance in Ω_k by a constant value (usually chosen between 1.0 and 2.0)[9].

Several definitions for these parameters can be found in the bibliography on the issue: Belystchko *et al.*[9] suggest

$$c = \alpha c_i, \qquad 1 \leq \alpha \leq 2, \qquad c_i = \max\|x_j - x_i\|, \qquad \forall\ j \in S_j \tag{27}$$

where S_j is the minimum set of neighbouring points of x_i which construct a polygon surrounding it, and Oñate[7] and Hegen[24] propose parameter c proportional to domain of influence d_{max}

$$c = \alpha d_{max} \qquad \alpha = 0.25 - 0.50 \tag{28}$$

Note that if $d_{max} \to \infty$ in (25) and (26), then the weight function value tends to unity and so, the standard least square approach is recovered.

In the following examples presented in this paper, the gaussian weighting function have been used. For this reason a graphical representation of it is given in figures 1 and 2 for different values of the required parameters.

2.4 Shape Functions and Derivatives

Shape functions can be obtained from equations (14), (15), (19) and (21). In figure 3 we represent the shape functions for different orders of the base functions in the 1D case. It is also possible to deduce analytical expressions by using constant, linear and quadratic base interpolating functions in 1D and 2D cases[25].

It must be noted that obtaining shape functions within a subdomain requires the computation and the inversion of matrix $\boldsymbol{A}$ at every point $\boldsymbol{x}$. This process is improved by using normalized coordinates (7), because the ill-conditioning of this matrix is avoided for some practical cases.

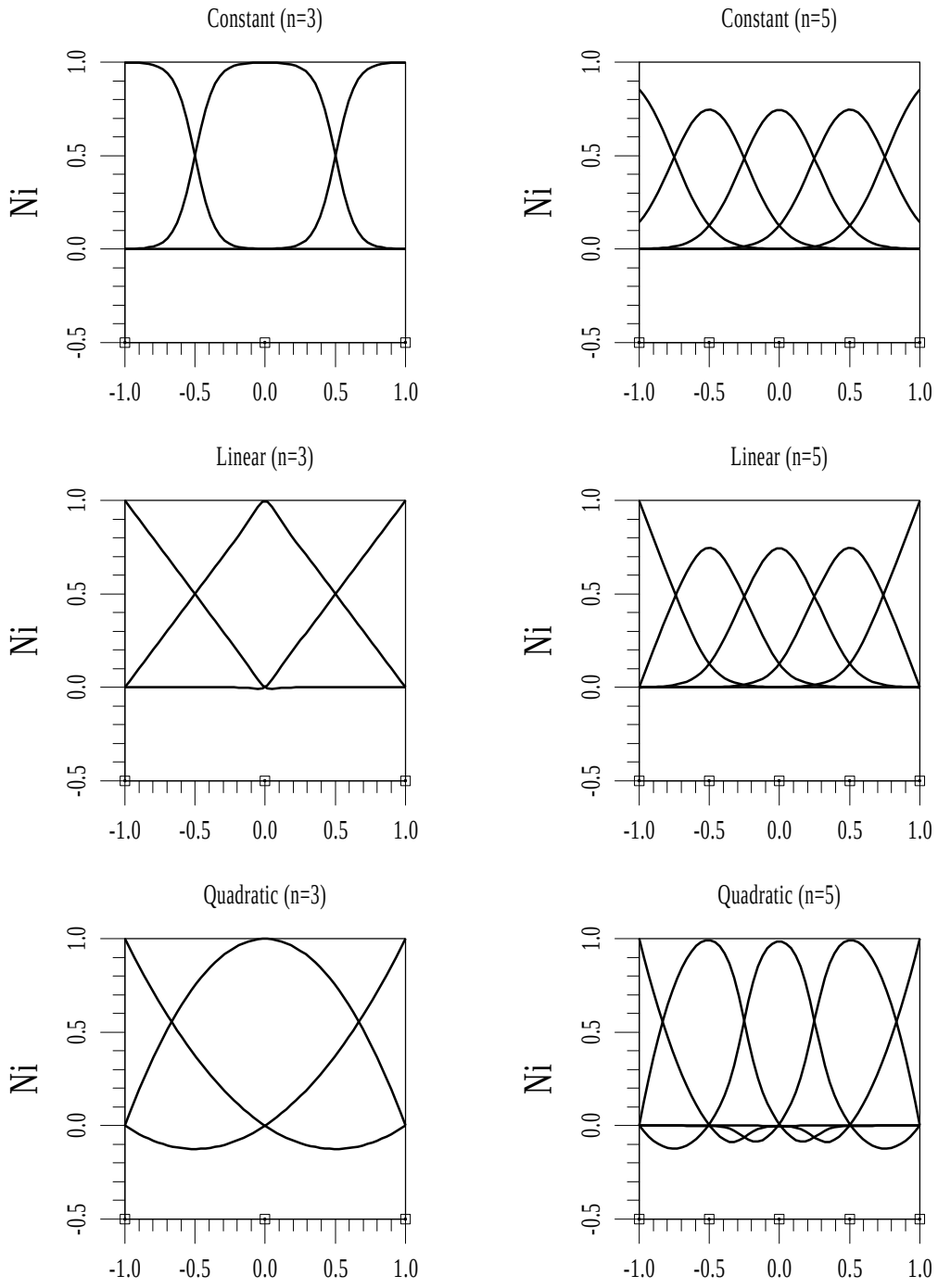

Figure 3.- Shape functions obtained by using constant, linear and quadratic base interpolating functions respectively for the 1D case, with $n = 3$ and $n = 5$ points of the subdomain (nodal points are marked).

However, obtaining analytical expressions for derivatives of shape functions up to an arbitrary order is unaffordable in practice. Therefore, derivatives must be performed by direct derivation of expression (21). For example, first and second derivatives of the shape functions for 1D problems result in,

$$\begin{aligned} \frac{d\boldsymbol{N}^t(x)}{dx} &= \frac{d\boldsymbol{p}^t(\xi_j)}{dx}\boldsymbol{C}(x) + \boldsymbol{p}^t(\xi_j)\frac{d\boldsymbol{C}(x)}{dx} \\ \frac{d^2\boldsymbol{N}^t(x)}{dx^2} &= \frac{d^2\boldsymbol{p}^t(\xi_j)}{dx^2}\boldsymbol{C}(x) + \boldsymbol{p}^t(\xi_j)\frac{d^2\boldsymbol{C}(x)}{dx^2} + 2\frac{d\boldsymbol{p}^t(\xi_j)}{dx}\frac{d\boldsymbol{C}(x)}{dx} \end{aligned} \tag{29}$$

being

$$\begin{aligned} \frac{d\boldsymbol{C}(x)}{dx} &= \boldsymbol{C}(x)\boldsymbol{W}^{-1}(x)\frac{d\boldsymbol{W}(x)}{dx}(\boldsymbol{I} - \boldsymbol{P}^t(\xi_j)\boldsymbol{C}(x)) \\ \frac{d^2\boldsymbol{C}(x)}{dx^2} &= -2\boldsymbol{C}(x)\boldsymbol{W}^{-1}(x)\frac{d\boldsymbol{W}(x)}{dx}\boldsymbol{P}^t(\xi_j)\frac{d\boldsymbol{C}(x)}{dx} + \\ &\quad \boldsymbol{C}(x)\boldsymbol{W}^{-1}(x)\frac{d^2\boldsymbol{W}(x)}{dx^2}(\boldsymbol{I} - \boldsymbol{P}^t(\xi_j)\boldsymbol{C}(x)) \end{aligned} \tag{30}$$

where matrices $\boldsymbol{P}$, $\boldsymbol{W}(x)$ $\boldsymbol{C}(x)$ are given by (16), (17) and (19), and $\boldsymbol{I}$ is the identity matrix.

Derivatives in 2D and 3D cases or high order ones may be obtained in analogous way as (29) and (30).

3. STATEMENT OF DISCRETIZED EQUATIONS

The selection of test functions in the general varational form (3) allows to derive different formulations. In the examples presented in this paper a point collocation method has been implemented, in order to take advantage of the meshless character of the approximation[20]. Other approaches based on integral methods have been proposed[15,16,18], but require some kind of auxiliar grid to evaluate the resulting integrals.

The point collocation scheme ($\Psi_i = \widehat{\Psi}_i = \widehat{\widehat{\Psi}}_i = \delta_i$ in expression (3), where δ_i is the Dirac delta) leads to the set of equations,

$$\begin{aligned} [A(\hat{u})]_i - b_i = 0 \quad &\text{in} \quad \Omega \\ [B(\hat{u})]_i - t_i = 0 \quad &\text{in} \quad \Gamma_t \\ \hat{u}_i - u_p = 0 \quad &\text{in} \quad \Gamma_u \end{aligned} \tag{31}$$

Now, if function $\hat{u}$ is approximated by linear combination (4) of the shape functions (21) the previous system of equations may be written in the standard form as,

$$\boldsymbol{K}\boldsymbol{u}^h = \boldsymbol{f} \tag{32}$$

where coefficient matrix $\boldsymbol{K}$ is banded (but not necessary symmetric), $\boldsymbol{f}$ is also known (contains the contributions from terms b and t and prescribed values u_p), and $\boldsymbol{u}^h$ contains the unknown values of the function evaluated in nodal points[20].

The validation of this moving least square method with a point collocation approach has been succesfully performed for different numerical tests[25]. Furthermore, Oñate *et al.*[7,8,20] have applied this method with promising results to the solution of problems in fluid mechanics. As we present in the next section, the meshless character of this formulation may represent an important improvement in the treatment of some problems in electrical engineering like the grounding analysis.

4. APPLICATION TO GROUNDING ANALYSIS

A safe grounding system has to guarantee the integrity of equipments and the continuity of the service under fault conditions —providing means to carry and dissipate electrical currents into the ground—, and to safeguard that persons working or walking in the surroundings of the grounded installation are not exposed to dangerous electrical shocks. To achieve these goals, the equivalent electrical resistance of the system must be low enough to assure that fault currents dissipate mainly through the grounding grid into the earth, while maximum potential differences between close points on the earth surface must be kept under certain tolerances (step, touch and mesh voltages)[1].

Physical phenomena underlying fault currents dissipation into the earth can be modelled by means of Maxwell's Electromagnetic Theory [26]. Constraining the analysis to the obtention of the electrokinetic steady-state response, and neglecting the inner resistivity of the earthing electrode, the 3D problem associated to an electrical current derivation to earth can be written as

$$\begin{gathered} \mathbf{div}\boldsymbol{\sigma} = 0, \qquad \boldsymbol{\sigma} = -\underline{\underline{\boldsymbol{\gamma}}}\,\mathbf{grad}V \ \text{ in } \ E; \\ \boldsymbol{\sigma}^t\boldsymbol{n}_E = 0 \ \text{ in } \ \Gamma_E; \quad V = V_\Gamma \ \text{ in } \ \Gamma; \quad V \longrightarrow 0, \ \text{ if } \ |\boldsymbol{x}| \to \infty; \end{gathered} \tag{33}$$

where E is the earth, $\underline{\underline{\boldsymbol{\gamma}}}$ its conductivity tensor, Γ_E the earth surface, $\boldsymbol{n}_E$ its normal exterior unit field and Γ the electrode surface[2,3]. Thus, when the electrode attains a voltage V_Γ (Ground Potential Rise or GPR) relative to a distant grounding point, the solution to this problem gives the potential V and the current density $\boldsymbol{\sigma}$ at an arbitrary point $\boldsymbol{x}$. Further assumption $V_\Gamma = 1$ is not restrictive at all, since V and $\boldsymbol{\sigma}$ are proportional to V_Γ.

For some practical purposes, the assumption of homogeneous and isotropic soil can be considered accurate[1], and the tensor $\underline{\underline{\boldsymbol{\gamma}}}$ can be substituted by a meassured apparent scalar conductivity γ. Otherwise, a multi-layer model (representing the ground as stratified into two or more layers of appropriate thickness, each one with a different value of γ) could be accepted without risking a serious calculation error[27]. Although the kind of techniques described in this paper can be applied to other soil models, examples presented in this paper are restricted to uniform soil models which earth surface is

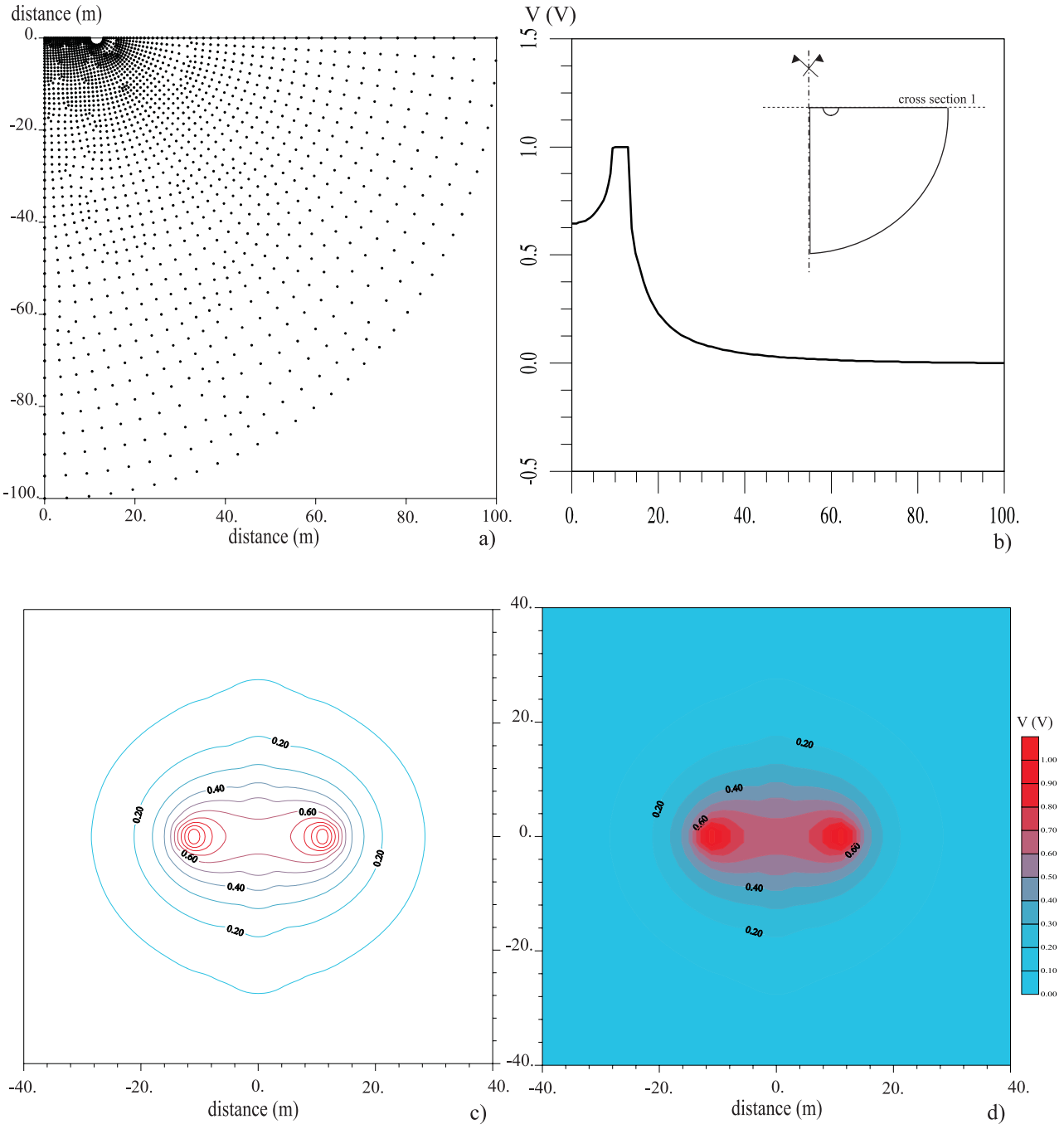

Figure 4.- Toroidal electrode in an infinite domain: a) Distribution of nodal points (npoin=1699), b) Potential profile along cross section 1, c) Contour lines around the electrode, d) Potential distribution around the electrode.

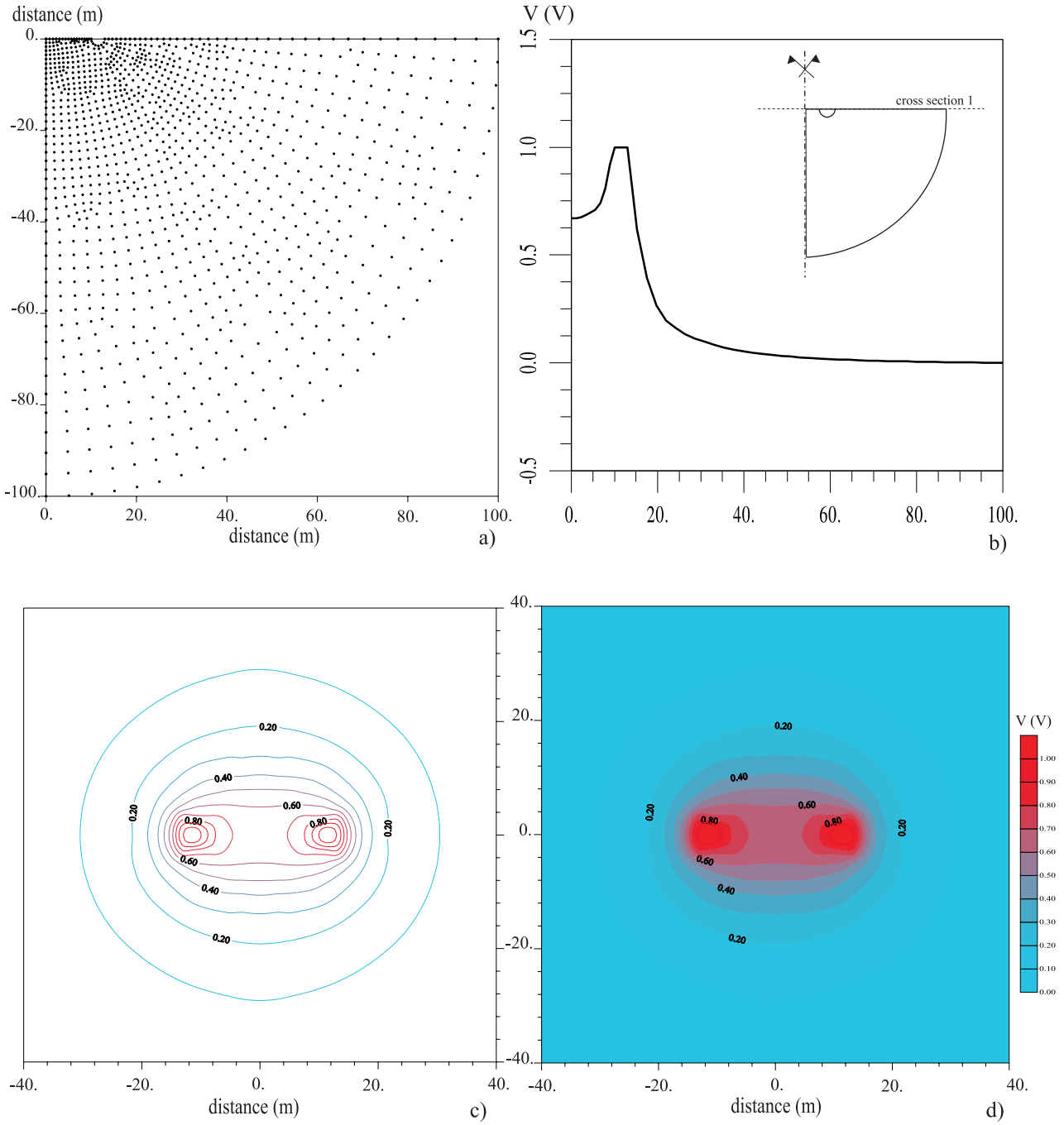

Figure 5.- Toroidal electrode in an infinite domain: a) Distribution of nodal points (npoin=1089), b) Potential profile along cross section 1, c) Contour lines around the electrode, d) Potential distribution around the electrode.

horizontal. Hence, problem (33) can be written in terms of the Neumann Exterior Problem[3]:

$$\Delta V = 0 \ \text{ in } \ E, \ \ \frac{dV}{dn_E} = 0 \ \text{ in } \ \Gamma_E, \ \ V = V_\Gamma \ \text{ in } \ \Gamma, \ \ V \longrightarrow 0, \ \ \text{if } \ |\boldsymbol{x}| \to \infty. \quad (34)$$

On the basis of this model for homogeneous and isotropic soils, we derived a numerical formulation based on the Boundary Element Method, which has been succesfully applied to the analysis of large grounding systems[2,3]. Recently, we have developed a new boundary element approach for earthing grids embedded in stratified soils, which feasibility has been demonstrated with its application to the practical case of a grounding system in a two-layer soil[5,28]. In cases in which we are interested to analyse earthing systems buried in more stratified soils or heterogeneous, the application of Boundary Element approaches implies a considerable computational effort.

On the other hand, the use of standard numerical techniques, such as finite elements, requires the discretization of domain E, the generation of a very complicated mesh of elements and the obtention of sufficiently accurate results would imply an extremely high (out of range) computational effort[3,4]. For these reasons, we have turned our attention to investigate the applicability of numerical formulations based on meshless methods for the solution of this problem.

The moving least square method with a point collocation approach presented in this paper has been applied to two test problems of grounding systems formed by a toroidal electrode. Due to the axial symmetry of the problem, solution can be obtained by using a 2D model.

The first example we present is a numerical test performed for a toroidal electrode in an infinite domain. The interior diameter of the ring is 20 m and the electrode diameter is 3 m. This case has been solved with two different point distributions for 1699 points and 1089 points obtained by means of the program GEN4U[29]. The base interpolating functions used are linear and all subdomains contain at least five points. Figures 4 and 5 show the nodal point distribution, the potential profile along a line, contour lines around the electrode and the potential distribution around it.

These numerical results agree significantly with those obtained by using a very dense point distribution and with results of a finite element program. Furthermore, the use of quadratic base interpolating functions allows to obtain more accurate results with a very acceptable computing effort.

The second example considered is the case of a toroidal electrode horizontally buried to a depth of 7 m. The interior diameter of the ring is 20 m and the electrode diameter is 3 m. This problem has been solved with two different point distributions with 1485 points and 3019 points also obtained by means of GEN4U[29]. As in the previous case, the base interpolating functions chosen are linear and a minimum of five points have been used in all subdomains. Figures 6 and 8 show the nodal point distributions and potential profiles along different lines. In figures 7 and 9, we represent the contour lines and the potential distribution around the electrode.

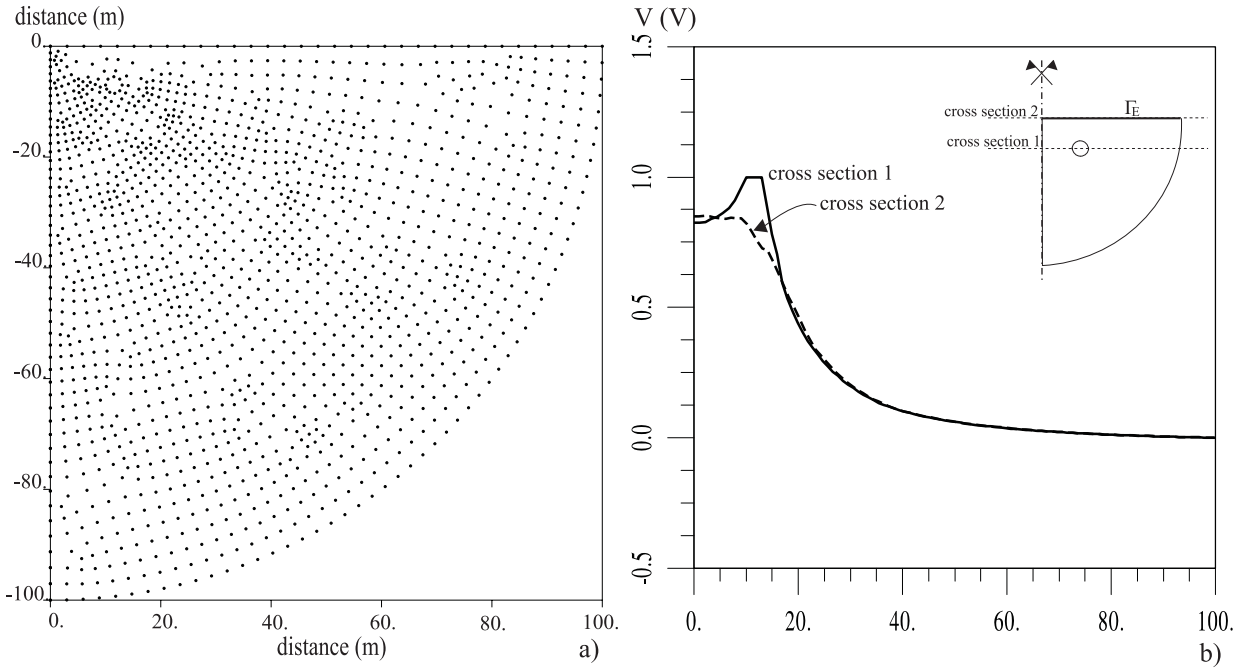

Figure 6.- Toroidal electrode buried to a depth of 7 m: a) Distribution of nodal points (npoin=1485), b) Potential profiles along cross section 1 and section 2 (earth surface Γ_t).

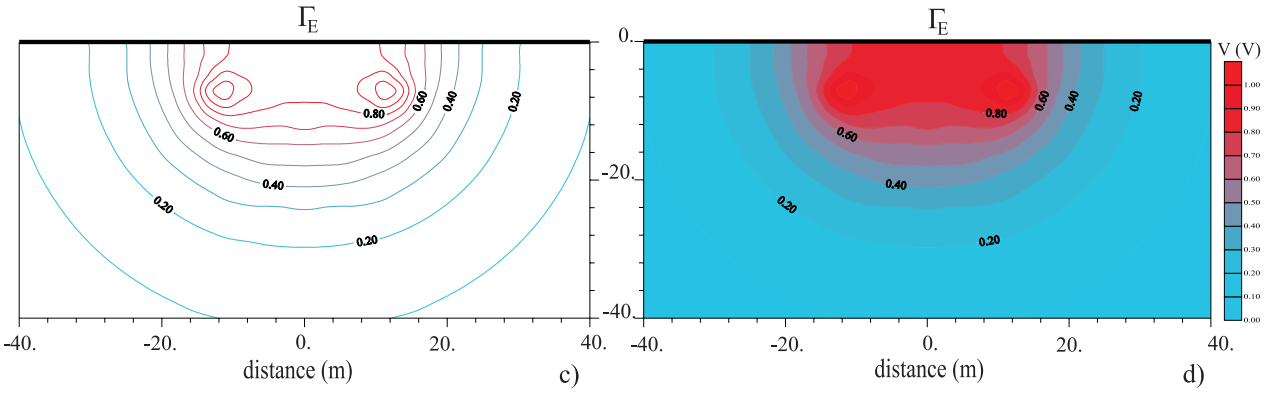

Figure 7.- Toroidal electrode buried to a depth of 7 m: c) Contour lines around the electrode, d) Potential distribution around the electrode.

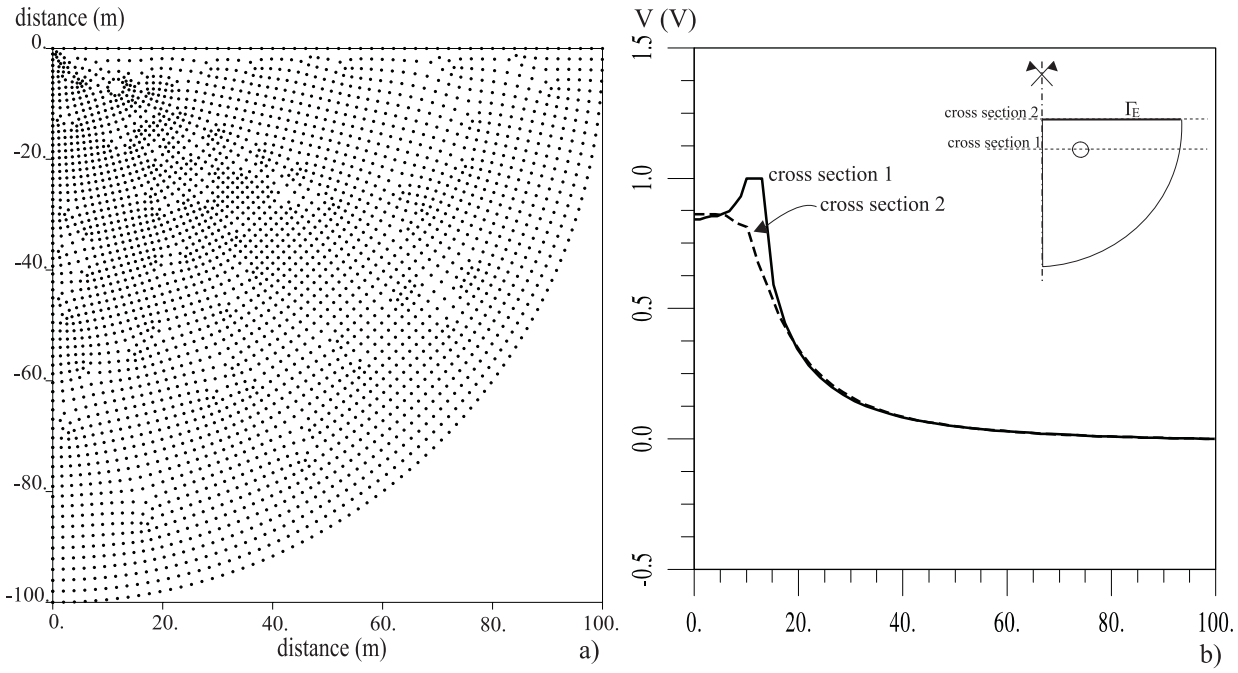

Figure 8.- Toroidal electrode buried to a depth of 7 m: a) Distribution of nodal points (npoin=3019), b) Potential profiles along cross section 1 and section 2 (earth surface Γ_s).

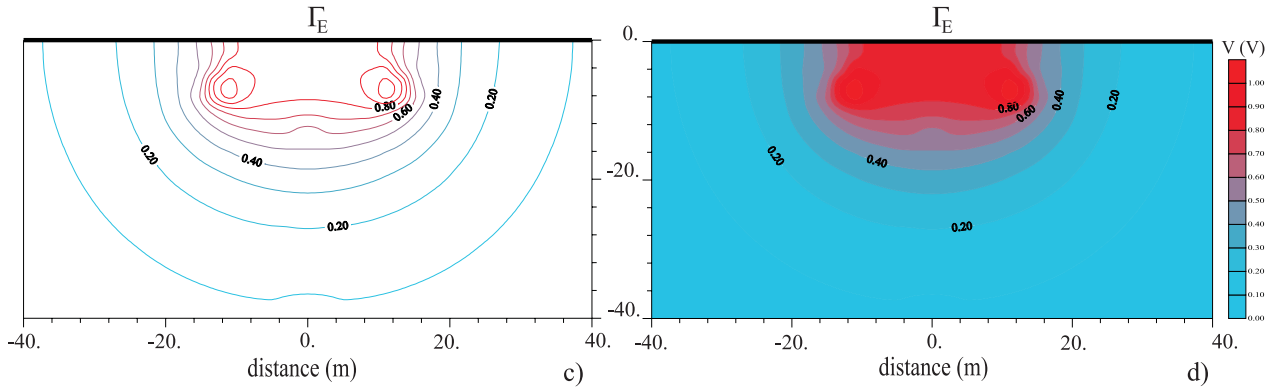

Figure 9.- Toroidal electrode buried to a depth of 7 m: c) Contour lines around the electrode, d) Potential distribution around the electrode.

5. CONCLUSIONS

A moving least square interpolation method with a point collocation approach has been presented. This method takes advantage of the fact that no auxiliary mesh is required, and so, it is possible to obtain the solution to boundary value problems from a finite set of points of the domain.

Meshless character of these methods may represent an important improvement in the computational analysis of some problems in the electrical engineering field, in which the use of standard numerical techniques (such as finite elements) is precluded due to large computational efforts required in the discretization process. An example of these engineering applications is the analysis and design of grounding systems of electrical installations.

In this paper, the MLS formulation has been applied to the solution of two test cases of grounding analysis, consisting of toroidal electrodes. Although further study and development are still required in order to assess the practical aspects of this method, first results obtained for different distributions of points are very promising requiring a low computational cost. More accurate results are possible to obtain by using dense point distributions or by means of higher order base interpolating functions, although in these cases the computing effort can significantly increase.

ACKNOWLEDGEMENTS

This work has been partially supported by the power company "Unión Fenosa", by research fellowships of the R&D General Secretary of the "Xunta de Galicia" and the University of La Coruña, and by the company "Fecsa".

6. REFERENCES

[1] ANSI/IEEE Std.80, *Guide for Safety in AC Substation Grounding*, IEEE Inc., New York (1986).

[2] Navarrina F., Colominas I., Casteleiro M., *Analytical integration techniques for earthing grid computation by boundary element methods*, International Congress on Numerical Methods in Engineering and Applied Sciences, II, 1197-1206. Concepción, (Chile) (1992).

[3] Colominas I., *Cálculo y Diseño por Ordenador de Tomas de Tierra en Instalaciones Eléctricas: Una Formulación Numérica basada en el MEC.*, PhD Thesis E.T.S.I.C.C.P, La Coruña (1995).

[4] Colominas I., Navarrina F., Casteleiro M., *A Boundary Element Numerical Approach for Earthing Grid Computation*, Advances in Engineering Software (in press).

[5] Colominas I., Aneiros J., Navarrina F., Casteleiro M., *A Boundary Element Numerical Approach for Substation Grounding in a Two Layer Earth Structure*, Advances in Computational Engineering Science, Section "Recent Developments in Boundary Element Method", 756–761, S.N. Atluri, G. Yagawa (Editors); Tech Science Press, Atlanta (1997).

[6] Belystchko T., Krongauz Y.,, Organ D., Krysl P., *Meshless methods: An overview and recent developments*, Computer Methods in Applied Mechanics and Engineering, vol 139, 3-48 (1996).

[7] Oñate E., Idelsohn S., Zienkiewicz O.C., Taylor R.L., *A finite point method in computational mechanics. Applications to convective transport and fluid flow*, International Journal for Numerical Methods in Engineering (1996).

[8] Oñate E., Idelsohn S., Zienkiewicz O.C., *Finite Point Methods in computational mechanics*, Research Report 67, CIMNE, Barcelona (1995).

[9] Belystchko T., Gu L., Lu Y.Y., *Element Free Galerkin Methods*, International Journal for Numerical Methods in Engineering, vol 37, 229-256 (1994).

[10] Liszka T., *An Interpolation Method for an irregular net of nodes*, International Journal for Numerical Methods in Engineering, vol 20, 1599-1612 (1984).

[11] Lucy L., *A Numerical Approach to Testing the fission Hypothesis*, Astron. Journal, vol 82, 1013-1024 (1977).

[12] Monaghan J.J., *Why Particle Methods Work*, SIAM J. Sci. Stat. Comp., vol 3, 422-433 (1982).

[13] Liu W.K., Li S., Belystchko T., *Moving least square Reproducing Kernel Methods. Part I: Methodology and convergence*, Computer Methods in Applied Mechanics and Engineering, vol 143, 113-154 (1997).

[14] Nayroles B., Touzot G., Villon P., *Generalizing the Finite Element Method: Diffuse Approximations and Diffuse Elements*, Computational Mechanics, vol 10, 307-318 (1992).

[15] Belystchko T., Organ D., Krongauz Y., *A coupled Finite Element-Element Free Galerkin Method*, Computational Mechanics, vol 17, 186-195 (1995).

[16] Liu W.K., Jun S., Zhang Y.F., *Reproducing Kernel Particle Methods*, International Journal for Numerical Methods in Fluids, vol 20, 1081-1106 (1995).

[17] Liu W.K., Chen Y., *Wavelet and Multiple Scale Reproducing Kernel Particle Methods*, International Journal for Numerical Methods in Fluids, vol 21, 901-931 (1995).

[18] Duarte C.A., Oden J.T., *A new meshless method to solve Boundary-Value Problems*, Proceedings of the XVI CILAMCE-Iberian Latin American Conference on Computational methods for engineering, Curitiba, Brazil, 90-99, R.D.Ed. (1995).

[19] Duarte C.A., Oden J.T., *Hp Clouds-A meshless method to solve Boundary Value Problems*, Technical Report95-05, TICAM, The University of Texas at Austin (1995).

[20] Oñate E., Idelsohn S., Zienkiewicz O.C., Taylor R.L., Sacco C., *A stabilized finite point method for analysis of fluid mechanics problems*, Computer Methods in Applied Mechanics and Engineering, vol 139, 315-346 (1996).

[21] Hughes, T.J.R., *The Finite Element Method*, Prentice Hall, New Jersey (1987).

[22] Liszka T., Duarte C.A., Tworzydlo W.W, *hp-Meshless cloud method*, Computer Methods in Applied Mechanics and Engineering, vol 139, 263-288 (1996).

[23] Taylor R.L., Idelsohn S., Zienkiewicz O.C., Oñate E., *Moving Least Square Approximation for solution of differential equations*, Research Report 74, CIMNE, Barcelona (1995).

[24] Hegen D., *Element Free Galerkin Methods in combination with finite element approaches*, Computer Methods in Applied Mechanics and Engineering, vol 135, 143-166 (1996).

[25] Chao M., *Introducción a los Métodos Numéricos sin Malla: fundamentación y desarrollo de formulaciones de mínimos cuadrados ponderados*, Research Report. E.T.S.I.C.C.P. (1997).

[26] Durand E., *Électrostatique*, Masson Ed. Paris (France) (1966).

[27] Heppe R.J., *Computation of potential at surface above an energized grid or other electrode, allowing for non-uniform current distribution*, EEE Trans. P.A.S., Vol. 98, No. 12, 1978–1988 (1979).

[28] Colominas I., Navarrina F., Casteleiro M., Aneiros J., *A BEM Formulation for Computational Design of Grounding Systems in Stratified Soils*, Proceedings of "Fourth World Congress on Computational Mechanics", Buenos Aires, Argentina (1998).

[29] Sarrate J., *Modelización numérica de la interacción fluido-sólido rígido: Desarrollo de algoritmos, generación de mallas y adptabilidad*, PhD Thesis E.T.S.I.C.C.P, Barcelona (1996).